VOLUME 121, NUMBER 48
DECEMBER 8, 1999

JOURNAL OF THE AMERICAN CHEMICAL SOCIETY

Radical Cation Transport and Reaction in RNA/DNA Hybrid Duplexes: Effect of Global Structure on Reactivity

Valerie Sartor, Paul T. Henderson, and Gary B. Schuster*

Contribution from the Department of Chemistry and Biochemistry, Georgia Institute of Technology, Atlanta, Georgia 30332-0400

Received July 19, 1999

Abstract: A series of anthraquinone-linked DNA and DNA/RNA hybrid duplexes was prepared and examined to assess the effect of global structure on long-range charge transport. Spectroscopic and chemical evidence indicates that the DNA/RNA hybrid duplexes adopt an overall A-form-like structure. Irradiation of the covalently linked anthraquinone group injects a radical cation and leads to remote damage at GG steps, which is revealed as strand breaks by subsequent treatment with piperidine. Radical cation transport through the A-form hybrid duplex occurs, but the strand cleavage at GG steps in the hybrid is much less efficient than it is in duplex DNA. These findings are interpreted within the phonon-assisted polaron-like hopping model to show that the reaction of a radical cation with H_2O in the A-form helix is inhibited relative to this reaction in B-form DNA.

Introduction

DNA has been extensively examined as a medium for long-distance, one-dimensional charge transport.[1−7] It has been demonstrated definitively that radical cations (holes) can migrate 200 Å or more through duplex DNA.[8−10] The mechanism responsible for electron transfer in DNA has been a subject of intensive debate. A proposal that duplex DNA behaves like a "molecular wire"[6] has been modified,[11] and we have suggested an alternative model identified as phonon-assisted polaron-hopping.[9] A key tenet of this proposal is that dynamical structural variation of DNA controls the rate and efficiency of charge transport. In particular, the presence of a base radical cation causes a local distortion (the polaron) that migrates in DNA in response to thermal activation by phonons. We are examining a range of nucleic acid compounds to probe the generality of long-distance charge transport and the limits of the phonon-assisted polaron-hopping model. These studies are of general relevance to potential application of DNA as an anisotropic conductor in mesoscopic electronic devices.[12,13] We report herein the examination of an RNA/DNA hybrid duplex and a [DNA−RNA−DNA]/DNA chimeric duplex.

Injection of radical cations into DNA by chemical or physical means has been shown to cause reactions that lead to mutations.[14−16] Probing the transport and reactions of radical

(1) Holmlin, E. R.; Dandliker, P. J.; Barton, J. K. *Angew. Chem., Int. Ed. Engl.* **1997**, *36*, 2715−2730.
(2) Beratan, D. N.; Priyadarshy, S.; Risser, S. M. *Chem. Biol.* **1997**, *4*, 3−8.
(3) Steenken, S. *Biol. Chem.* **1997**, *378*, 1293−1297.
(4) Diederichsen, U. *Angew. Chem., Int. Ed. Engl.* **1997**, *36*, 2317−2319.
(5) Jortner, J.; Bixon, M.; Langenbacher, T.; Michel-Beyerle, M. E. *Proc. Natl. Acad. Sci. U.S.A.* **1998**, *95*, 12759−12765.
(6) Turro, N. J.; Barton, J. K. *J. Biol. Inorg. Chem.* **1998**, *3*, 201−209.
(7) Ratner, M. *Nature* **1999**, *397*, 480−481.
(8) Nunez, M.; Hall, D. B.; Barton, J. K. *Chem. Biol.* **1999**, *6*, 85−97.
(9) Henderson, P. T.; Jones, D.; Hampikian, G.; Kan, Y.; Schuster, G. B. *Proc. Natl. Acad. Sci. U.S.A.* **1999**, *96*, 8353−8358.
(10) Ly, D.; Sanii, L.; Schuster, G. B. *J. Am. Chem. Soc.* **1999**, *121*, 9400−9410.
(11) Wan, C.; Fiebig, T.; Kelly, S. O.; Treadway, C. R.; Barton, J. K.; Zewail, A. H. *Proc. Natl. Acad. Sci. U.S.A.* **1999**, *96*, 6014−6019.
(12) Okahata, Y.; Kobayashi, T.; Tanaka, K.; Shimomura, M. *J. Am. Chem. Soc.* **1998**, *120*, 6165−6166.
(13) Fink, H. W.; Schonenberger, C. *Nature* **1999**, *398*, 407−410.
(14) Demple, B.; Harrison, L. *Annu. Rev. Biochem.* **1994**, *63*, 915−948.
(15) Loft, S.; Poulsen, H. E. *J. Mol. Med.* **1996**, *74*, 297−312.

10.1021/ja9925406 CCC: $18.00
Published on Web 11/13/1999

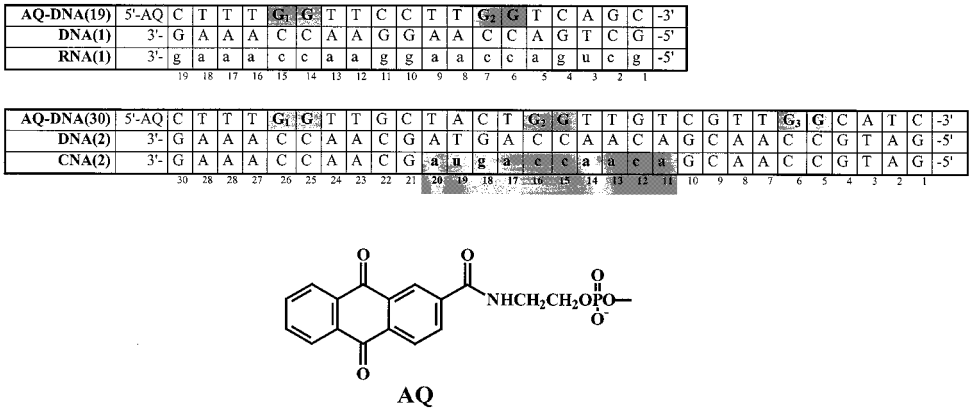

Figure 1. Sequences for the oligonucleotides and conjugates studied in this work. The lower case base symbols refer to ribose-containing structures; the upper case symbols are for deoxyribose-containing structures.

cations in RNA/DNA hybrid duplexes is important because they are key intermediates in replication, transcription, and reverse transcription. In addition, non-natural cellular hybridization between mRNA and a complementary DNA oligomer with subsequent cleavage of the RNA strand by RNase H is an essential strategy in antisense therapy.[17]

The X-ray crystal structures of RNA/DNA hybrid duplexes reveal almost pure A-form structures.[18,19] The solution conformations of several RNA/DNA hybrids of mixed sequence have been reported.[20−23] It is clear that the sugars of the RNA strand are locally in A conformation (C3′-*endo*), whereas those in the DNA strand have conformations more similar to those found for B-conformation (C2′-*endo*). Gyi and co-workers discovered that the stability and structure of RNA/DNA hybrids depend on the arrangement of bases.[20] In particular, hybrid duplexes containing purine-rich RNA strands are more stable and more A-like than hybrids with a pyrimidine-rich RNA strand. Assessment of circular dichroism (CD) spectra led Lesnik and Freier[22] to conclude that there is a continuum of hybrid conformers that are intermediate between A and B-forms. However, overall the hybrid duplexes are closer to A-form than the B-form, albeit with a narrower minor groove than RNA.[24,25]

The global structures of chimeric duplexes containing DNA/RNA regions in the solid state, determined by X-ray crystallography, and in solution, determined by NMR spectroscopy, are different. In the solid state, one ribonucleotide in the DNA strand transforms the entire duplex to the A-form;[19,26] but in solution the global structure remains B-form with only the ribose residue adopting a C3′-*endo* sugar pucker.[27] These different results are attributed to the effects of hydration and, perhaps, to crystal packing forces. Zhu and co-workers[28] used NMR spectroscopy to show that the helical properties of RNA/DNA segments are closer to A-form than to B-form. More recently, Nishizaki and co-workers[29] examined chimeric hybrid duplexes containing a central ribonucleotide region. They also report that its global structure is closer to that of A-form than to that of B-form. We employ RNA/DNA hybrid duplexes to assess the influence of global structure on the transport and reactions of radical cations.

We have developed a reliable synthetic strategy for coupling a tethered anthraquinone derivative (AQ, see Figure 1) covalently to the 5′-terminus of a DNA oligonucleotide. This attachment defines the AQ location and restricts its allowable interaction geometries. We have shown that the four-atom tether between the quinone group and the terminal phosphate of AQ is too short to permit intercalation in DNA.[30] Chemical, spectroscopic, and modeling data indicate that the anthraquinone is associated (end-capped) with the terminal base pair of DNA due primarily to stabilizing hydrophobic interactions.[31] We presume that the same forces will cause end-capping by AQ with the RNA/DNA hybrid.

Irradiation of the end-capped quinone leads to one electron oxidation of a neighboring base to its radical cation.[9,32] Migration of the radical cation through the DNA duplex is revealed by selective reaction at remote GG steps that is assayed by measuring strand cleavage of radiolabeled samples caused by treatment with piperidine.[33−36] Application of this technique to the study of the RNA/DNA hybrids demonstrates that radical cations can be transported through these structures, but the efficiency of transport and the observed reaction of the guanine radical cation are sensitive to the global structure of the nucleic acid.

(16) Cadet, J. *DNA Adducts: Identification and Significance*; Hemminiki, K., Dipple, A., Shiker, D. E., Kadlubar, F. F., Segerback, D. and Bartsch, H., Ed.; IARC: Lyon, France, 1994.
(17) Stein, C. A.; Cheng, Y.-C. *Science* **1993**, *261*, 1004−1021.
(18) Egli, M.; Usman, N.; Zhang, S.; Rich, A. *Proc. Natl. Acad. Sci., U.S.A.* **1992**, *89*, 534−548.
(19) Egli, M.; Usman, N.; Rich, A. *Biochemistry* **1993**, *32*, 3221−3237.
(20) Gyi, J. I.; Conn, G. L.; Lane, A. N.; Brown, T. *Biochemistry* **1996**, *35*, 12538−12548.
(21) Gyi, J. I.; Lane, A. N.; Conn, G. L.; Brown, T. *Nucleic Acids Res.* **1998**, *26*, 3104−3110.
(22) Lesnik, E. A.; Freier, S. M. *Biochemistry* **1995**, *34*, 10807−10815.
(23) Wang, A. H.-J.; Fujii, S.; van Boom, J. H.; van der Marel, G. A.; Boeckel, S. A. A.; Rich, A. *Nature* **1992**, *299*, 601−604.
(24) Fedoroff, O. Y.; Salazar, M.; Reid, B. R. *J. Mol. Biol.* **1993**, *233*, 509−523.
(25) Conn, G.; Brown, T.; Leonard, G. A. *Nucleic Acids. Res.* **1999**, *27*, 555−561.
(26) Ban, C.; Ramakrishnan, B.; Sundaralingam *J. Mol. Biol.* **1994**, *236*, 275−285.
(27) Jaishree, T. H.; van der Marel, G. A.; van Boom, J. H. *Biochemistry* **1993**, *30*, 10606−10613.
(28) Zhu, L.; Salazar, M.; Reid, B. R. *Biochemistry* **1995**, *34*, 2372−2380.
(29) Nishizaki, T.; Iwai, S.; Ohkubo, T.; Kojima, C.; Nakamura, H.; Kyogoku, Y.; Ohtsuka, E. *Biochemistry* **1996**, *35*, 4016−4025.
(30) Gasper, S. M.; Schuster, G. B. *J. Am. Chem. Soc.* **1997**, *119*, 12762−12771.
(31) Guckian, K. M.; Schweitzer, B. A.; Ren, R., X.-F.; Sheils, C. J.; Paris, P. L.; Tahmassebi, D. C.; Kool, E. T. *J. Am. Chem. Soc.* **1996**, *118*, 8182−8183.
(32) Gasper, S. M.; Armitage, B.; Hu, G. G.; Shui, X.; Yu, C.; Williams, L. D.; Schuster, G. B. *J. Am. Chem. Soc.* **1998**, *120*, 12402−12409.
(33) Ito, K.; Inoue, S.; Yamamoto, K.; Kawanishi, S. *J. Biol. Chem.* **1993**, *268*, 13221−13227.
(34) Saito, I.; Takayama, M.; Sugiyama, H.; Nakatani, K.; Tsuchida, A.; Yamamoto, M. *J. Am. Chem. Soc.* **1995**, *117*, 6406−6407.
(35) Hall, D. B.; Holmlin, R. E.; Barton, J. K. *Nature* **1996**, *382*, 731−735.
(36) Armitage, B. A.; Yu, C.; Devadoss, C.; Schuster, G. B. *J. Am. Chem. Soc.* **1994**, *116*, 9847−9859.

Table 1. Melting Temperatures for DNA- and RNA-containing Oligomers in °C

	DNA(1)	RNA(1)
DNA(19)	52.3	51.9
AQ-DNA(19)	57.0	56.8
	DNA(2)	CNA(2)
DNA(30)	56.9	45.8
AQ-DNA(30)	59.5	49.9

Results

(1) Construction of Hybridized AQ-Conjugates. Figure 1 shows the oligonucleotides prepared to assess long-range radical cation transport. AQ-DNA(19) is a 19-mer containing two GG steps and an AQ group linked to its 5′-end. DNA(1) is the complement to AQ-DNA(19). RNA(1), composed of 12 purines and 7 pyrimidines, has the same sequence of bases as DNA(1) except that T has been replaced by U. AQ-DNA(30) is a 30-mer with a 5′-linked AQ group. There are three GG steps distributed in AQ-DNA(30) to act as probes for radical cation migration. DNA(2) is the complement to AQ-DNA(30); it contains 19 purines and 11 pyrimidines. CNA(2) is a chimera also complementary to AQ-DNA(30). In CNA(2), the first 10 bases from the 5′-end are linked to deoxyriboses, the next 10 bases are formed from riboses, and the last 10 are linked to deoxyriboses. When AQ-DNA(30) is hybridized with CNA(2), GG_1, the closest GG step to the AQ, is part of a DNA/DNA duplex, GG_2 is located in a DNA/RNA hybrid duplex region, and GG_3 is part of a DNA/DNA duplex. These compounds were prepared by standard solid-phase synthetic methods, which have been previously described,[30] and were purified by HPLC.

(2) Characterization of Hybridized AQ-Conjugates. Thermal stabilization of the double-stranded nucleic acid oligomers by the AQ substituent is a good indication of interaction of the DNA bases with the anthraquinone group. This stabilization was assessed by measuring the melting temperatures (T_m) of the duplexes, Table 1. The T_m values were obtained from first derivative plots from the melting of DNA(19) and AQ-DNA(19) as part of duplexes formed by hybridization with DNA(1) or with RNA(1) monitored by the absorbance change at 260 nm. Since the RNA strand is purine-rich, the DNA/DNA duplex is expected to have only a slightly higher T_m than the DNA/RNA hybrid.[21,22,37] In fact, the T_m difference between the DNA and the hybrid is 0.4 °C.

These experiments also show that introduction of the AQ group causes an increase in T_m for the DNA/DNA duplex of 4.7 °C and for the RNA/DNA hybrid duplex of 4.9 °C. The similar increase in T_m for these two cases is evidence of a similar interaction for each duplex with the AQ. We assign this interaction to end-capping wherein π-electron contact between the anthraquinone group and the terminal base pair of the duplex is enforced by hydrophobic[31] and charge-transfer interactions. The results of melting experiments for DNA(30) are also summarized in Table 1. Interaction with the anthraquinone group stabilizes these duplex structures, too. Compared with the structures lacking the AQ group, T_m for AQ-DNA(30)/CNA(2) is increased by 4.1 °C and by 2.6 °C for AQ-DNA(30)/DNA(2). The chimeric hybrid duplex shows a single transition with T_m that is 10.4 °C below that of AQ-DNA(30)/DNA(2).

Circular dichroism spectroscopy is a useful tool in the examination of global DNA structure.[38,39] B-form DNA exhibits a characteristic CD spectrum, which differs significantly from the spectrum observed for A-form RNA.[40] In particular, the A-form has a negative band at 210 nm and a stronger positive band above 250 nm than does the B-form. Gray and coworkers[41] examined the CD spectroscopy of RNA/DNA hybrid duplexes and found that their appearance depends on the particular sequence. In some cases the CD spectra of the hybrid has a form similar to RNA, and in others the CD spectrum is more B-form-like. This supports the results from NMR spectroscopy that the oligomeric hybrids have ensembles of structures that are intermediate between A and B forms.

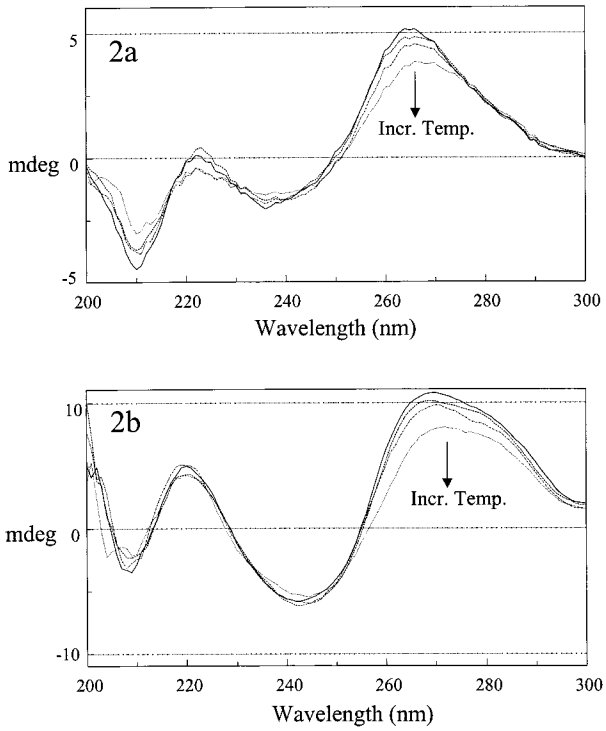

Figure 2. Circular dichroism spectra of DNA(19)/RNA(1), **2a** and AQ-DNA(30)/CNA(2), **2b** at various temperatures: (—) 20 °C, (- - -) 30 °C, (—•—•—) 40 °C, (•••) 50 °C. Samples contained 1 μM duplex oligonucleotide in 10 mM sodium phosphate buffer (pH = 7).

Figure 2a shows CD spectra of DNA(19)/RNA(1) recorded as a function of temperature between 20 and 50 °C in sodium phosphate buffer solution at pH = 7.0. At 20 °C, its form is typical of RNA/DNA hybrids, indicating an average global structure close to A-form. This spectrum changes as the temperature is increased to 50 °C in ways that are paralleled precisely by that of DNA(30)/CNA(2), which is shown in Figure 2b. At 20 °C, for both compounds, there are weak negative bands at ~210 nm and stronger positive bands above 250 nm. These features indicate, as expected, that the global structure of these hybrids are more A-like than B-like. At higher temperatures, the intensity of the 250 nm band decreases. This signals a change in the ensemble of conformations with the global structure becoming less A-like as the temperature is increased.

(3) Photochemistry of AQ-DNA hybrid duplexes. A sample of AQ-DNA(19) was labeled with ^{32}P at its 3′-terminus and hybridized with DNA(1). This sample was irradiated at 350 nm (only the anthraquinone absorbs) in the phosphate buffer solution

(37) Ratmeyer, L.; Vinayak, R.; Zhong, Y. Y.; Zon, G.; Wilson, W. D. *Biochemistry* **1994**, *33*, 5298−5304.
(38) Ivanov, V. I.; Minchenkova, L. E.; Schyolkina, A. K.; Poletayev, A. I. *Biopolymers* **1973**, *12*, 89−110.
(39) Gray, D. M.; Hung, S.-H.; Johnson, K. H. *Methods Enzymol.* **1995**, *246*, 19−36.
(40) Wells, B. D.; Yang, J. T. *Biochemistry* **1974**, *13*, 1317−1321.
(41) Hwung, S.-H.; Yu, Q.; Gray, D. M.; Ratliff, R. L. *Nucleic Acids Res.* **1994**, *22*, 4326−4334.

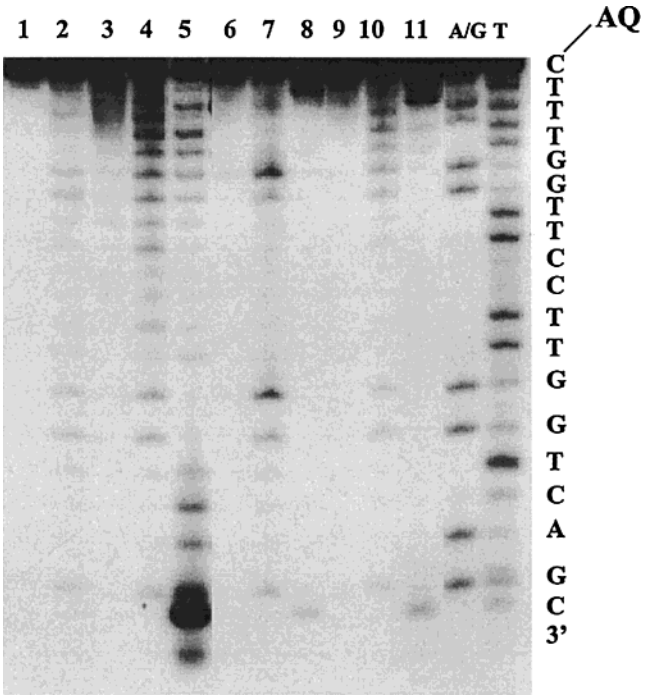

Figure 3. Autoradiogram demonstrating DNA cleavage in AQ-DNA(19), AQ-DNA(19)/DNA(1), and AQ-DNA(19)/RNA(1) as induced by irradiation of the linked anthraquinone (350 nm). Samples contained 5 μM single strand or duplex oligonucleotide and 6000 cpm ^{32}P-3′-end-labeled AQ-DNA(19) in 10 mM sodium phosphate buffer (pH = 7). Lane 1 is an unirradiated single-stranded AQ-DNA(19) control sample. Lane 2 is the same as lane 1 but treated with piperidine at 90 °C for 30 min. Lane 3 is an irradiated (30 min) AQ-DNA(19) sample with no piperidine treatment. Lane 4 is the same as lane 3 with piperidine treatment. Lane 5 is the same as lane 1, but with treatment by S1 nuclease for 30 min. Lanes 6−8 are the same as lanes 3−5, but with the AQ-DNA(19)/DNA(1) duplex. Lanes 9−11 are the same as lanes 3−5 but with the AQ-DNA(1)/RNA(1) hybrid duplex.

(pH = 7.0) at 25 °C for 30 min. After irradiation, the sample was treated with piperidine (90 °C, 30 min) and then analyzed by polyacrylamide gel electrophoresis (PAGE) and autoradiography. The results are shown in Figure 3, lane 7. As expected,[9,30] strand cleavage is seen at the two GG steps of AQ-DNA(19). For both the proximal GG_1 (closer to the AQ) and distal GG_2 step, cleavage at the 5′-G is more efficient than it is at the 3′-G. This behavior is characteristic of the reactions of radical cations in duplex DNA.[33−36] Irradiation of AQ-DNA(19)/RNA(1) under identical conditions gives a strikingly different result, Figure 3, lane 10. There is no measurable cleavage at the distal GG_2 above the background level (lane 2). Cleavage at the proximal GG_1 step is much weaker than it is in the DNA sample, and there is no 5′-G selectivity. Indeed, the reactions observed from irradiation of AQ-DNA(19)/RNA(1) seem to be localized around the AQ group. Irradiation at 35 °C gives a different result,[42] which parallels precisely the temperature dependence seen in the irradiation of DNA(30)/CNA(2). We performed a number of control experiments to assess the results from irradiation of AQ-DNA(19)/RNA(1).

We verified that AQ-DNA(19)/RNA(1) is present in solution as a duplex, since irradiation of single-stranded AQ-DNA(19) also leads to cleavage after piperidine treatment (Figure 3, lane 4). S1 nuclease selectively hydrolyzes single-stranded DNA.[43] Treatment of AQ-DNA(19) with this enzyme results in its extensive hydrolysis (lane 5) verifying that the AQ-substituent does not inhibit reaction. In contrast, the data in Figure 3 lanes 8 and 11 show that there is essentially no hydrolysis of AQ-DNA(19) by S1 nuclease when it is hybridized with DNA(1) or RNA(1), respectively. These results verify duplex stability under the reaction conditions for both cases.

The strand cleavage observed from irradiation might be intramolecular or intermolecular. Intermolecular reactions could result from the generation of a diffusible intermediate, such as singlet oxygen,[44−46] or by aggregation of the nucleic acid samples. These possibilities were excluded by experiments wherein the samples contain excess RNA(1) or DNA(1). Neither case shows a reduction in the cleavage efficiency. These observations verify that excitation of the attached anthraquinone causes strand cleavage.

Photolysis of 3′-radiolabeled AQ-DNA(30) hybridized with DNA(2) or with CNA(2) reveals critical features about the transport and reactions of radical cations in this RNA/DNA hybrid duplex. Irradiation of AQ-DNA(30)/DNA(2) for 1 h at 20 °C followed by piperidine treatment gives the expected 5′-G selective cleavage at each of the three GG steps of AQ-DNA(30). However, irradiation of AQ-DNA(30)/CNA(2) under these conditions gives essentially no cleavage at any of the GG steps. The reaction of AQ-DNA(30)/CNA(2) is surprisingly temperature dependent. Irradiation at 35 °C, Figure 4, results in piperidine-requiring strand cleavage selectively at the 5′-G of each of the three GG steps of DNA(30). Also shown in Figure 4 are the results from irradiation of AQ-DNA(30)/DNA(2) at 35 °C. As expected, the observed 5′-G selective cleavage of this compound falls off exponentially with the distance between the guanine and the AQ group (slope, $\gamma = -0.02_2$ Å^{-1}).[9,10] Although the overall efficiency is 40 times lower in the hybrid duplex, the reaction pattern is the same as it is for AQ-DNA(30)/DNA(2). Essentially parallel results are obtained from irradiation of AQ-DNA(19)/RNA(1) at 35 °C.[42] Control experiments, described above, verify that these reactions are intramolecular.

Comparison of the results from irradiation of AQ-DNA(30) hybridized with DNA(2) and with CNA(2) is very informative. Figure 5 shows the efficiency of strand cleavage (normalized so that $GG_1 = 1.0$) at each of the GG steps of AQ-DNA(30) for both its DNA complement and the chimeric hybrid duplex. The efficiency of reaction at GG_3 is surprisingly similar in both cases. This shows that transport of the radical cation through the hybrid duplex region is not significantly diminished compared with charge migration in duplex DNA. However, the yield of strand cleavage at GG_2, which is in the hybrid duplex region, is less than it is in duplex DNA. Clearly, the radical cation is trapped less effectively when it is in the hybrid region.

Discussion

Consideration of the behavior of radical cations in nucleic acids can be divided conceptually into three categories: charge injection (oxidation); migration; and reaction.[5] This study of DNA/RNA hybrid duplexes reveals new aspects of each category.

(1) Charge Injection. Introduction of radical cations (charge injection) into DNA occurs in natural metabolic processes[47] by

(42) The autoradiogram of the gel showing the temperature dependence is included as Supporting Information to this paper.

(43) Schoenberg, D. R.; Cunningham, K. S. *Methods* **1999**, *17*, 60−73.
(44) Blazek, E. R.; Peak, J. G.; Peak, M. J. *Photochem. Photobiol.* **1989**, *49*, 607−613.
(45) Floyd, R. A.; West, M. S.; Eneff, K. L.; Schneider, J. E. *Archiv. Biochem. Biophys.* **1989**, *273*, 106−111.
(46) Devasagayam, T. P. A.; Steenken, S.; Obendorf, M. S. W.; Schulz, W. A.; Sies, H. *Biochemistry* **1991**, *30*, 6283−6289.
(47) Bohr, V. A.; Dianov, G. L. *Biochimie* **1999**, *81*, 155−160.
(48) Teoule, R. *Int. J. Radiat. Biol.* **1987**, *51*, 573−589.

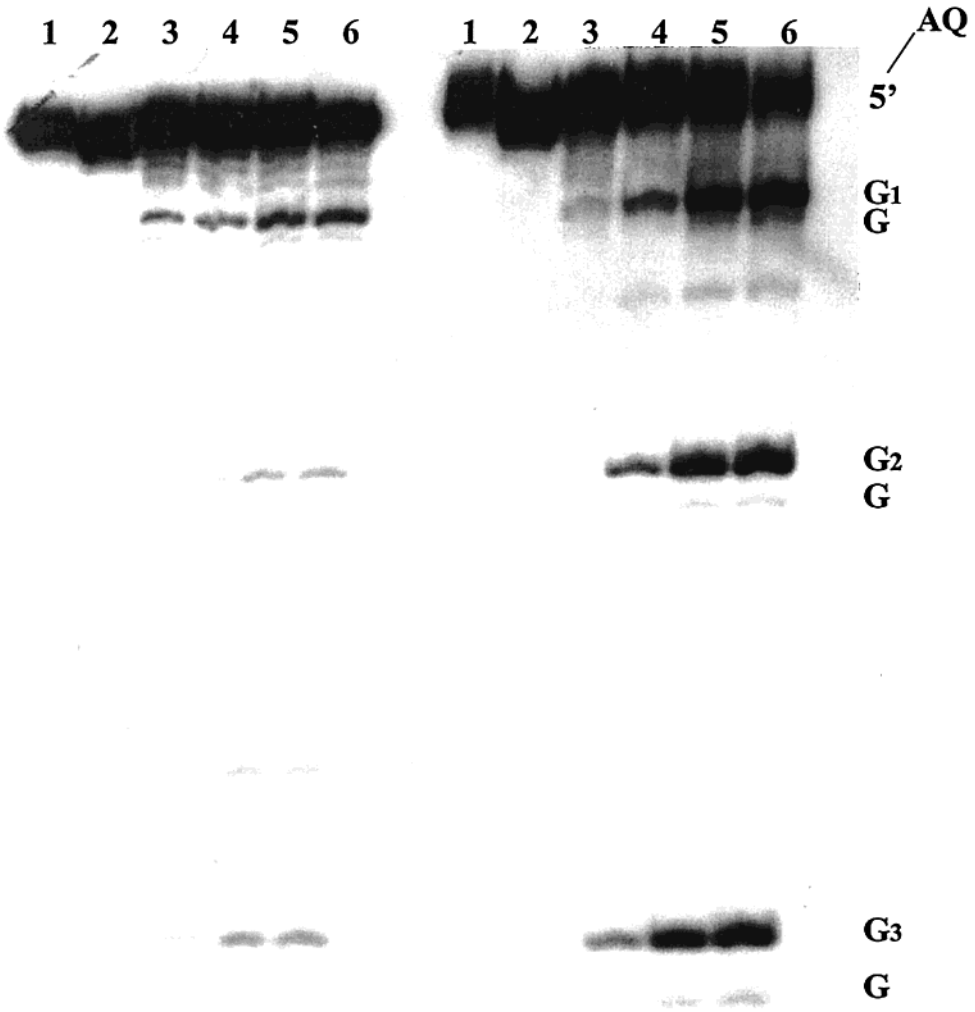

Figure 4. Autoradiograms demonstrating DNA cleavage in: (left gel)AQ-DNA(30)/CNA(2) and (right gel) AQ-DNA(30)/DNA(2) as induced by irradiation of the linked anthraquinone (350 nm) at 35 °C. Samples contained 5 μM duplex oligonucleotide and 6000 cpm ^{32}P-3′-end-labeled AQ-DNA(30) in 10 mM sodium phosphate buffer (pH = 7). Lane 1 is for unirradiated duplex control sample. Lane 2 is the same as lane 1 but treated with piperidine treatment at 90 °C for 0.5 h. Lane 3 is for irradiated (2 h) duplex samples with no piperidine treatment. Lanes 4, 5, and 6 are for irradiated duplex samples, 0.5, 1, and 2 h, respectively, with piperidine treatment at 90 °C for 0.5 h.

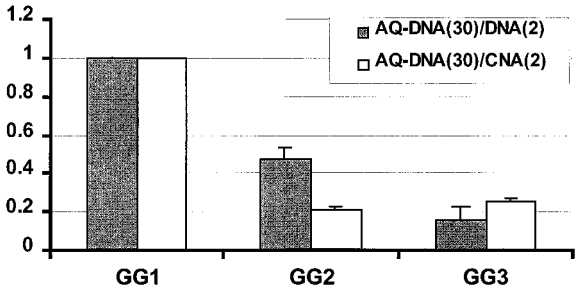

Figure 5. The relative efficiency of strand cleavage (normalized so that $GG_1 = 1.0$) at each of the GG steps of AQ-DNA(30) for both its DNA complement and the chimeric hybrid duplex. Standard deviations of independent replicates are indicated for cleavage at GG_2 and GG_3

exposure to ionizing radiation,[48] by light-induced single electron transfer,[33,49,50] and by reactions of specially modified nucleotides.[51,52] The method of charge injection can affect the outcome of the reaction. For example, ionizing radiation generally produces positive and negative charge centers, distributed randomly over the DNA, and other reactive species such as hydroxyl radical.[53] Interactions between these intermediates can influence the chemical outcome. Similarly, charge injection by reaction of a modified nucleotide may introduce a defect (a nick, for example) in the DNA structure.[54] An advantage of charge injection by light-induced single-electron transfer is that this process can be initiated with little structural perturbation to the DNA.

A covalently attached AQ group at a 5′-end of DNA seems to be an ideal system for introduction of radical cations. Since the anthraquinone group is not intercalated, it does not distort the native structure. Nevertheless, electronic contact between the excited-state end-capped quinone and the nucleic acid bases is sufficient to allow electron transfer. The excited singlet state of anthraquinone derivatives generally intersystem cross rapidly to the triplet.[55] Electron transfer from a base to the triplet quinone is thermodynamically favorable[3,56] and will generate a

(49) Candeias, L. P.; Steenken, S. *J. Am. Chem. Soc.* **1993**, *115*, 2437−2440.
(50) Stemp, E. D. A.; Holmlin, R. E.; Barton, J. K. *Nature* **1996**, *382*, 731−735.
(51) Giese, B.; Dussy, A.; Meggers, E.; Petretta, M.; Schwitter, U. *J. Am. Chem. Soc.* **1997**, *119*, 11130−11131.
(52) Gugger, A.; Batra, R.; Rzadek, P.; Rist, G.; Giese, B. *J. Am. Chem. Soc.* **1997**, *119*, 8740−8741.
(53) Pogozelski, W. K.; Xapsos, M. A.; Blakely, W. F. *Radiat. Res.* **1999**, *151*, 442−448.
(54) Meggers, E.; Michel-Beyerle, M. E.; Giese, B. *J. Am Chem. Soc.* **1998**, *120*, 12950−12955.
(55) Loeff, I.; Rabani, J.; Treinin, A.; Linschitz, H. *J. Am. Chem Soc.* **1993**, *115*, 8933−8942.

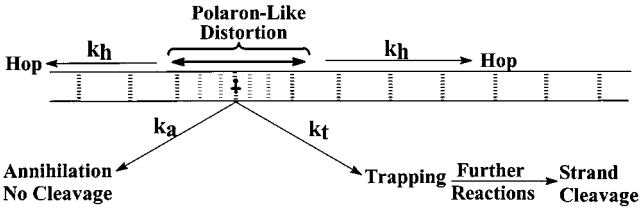

Figure 6. Schematic representation of the phonon-assisted polaron-hopping model for charge transport.

radical ion pair in an overall triplet state. An advantage of this chain of events is that ion pair annihilation (back electron transfer) is slow from the triplet, and this provides time for other reactions to occur. We have observed the anthraquinone radical anion spectroscopically and monitored its reaction with O_2 to form superoxide ($O_2^{-\bullet}$).[36] An important consequence of this sequence of reactions is that it injects a base radical cation in DNA whose lifetime is not limited by back electron transfer to a paired radical anion. Further, since the anthraquinone is regenerated, relatively inefficient reactions of the radical cation can be detected.

The interaction of the AQ group with the RNA/DNA hybrid duplexes is revealed by examination of their thermal stability to be essentially identical to that with duplex DNA. This supports our earlier conclusion of end-capping rather than intercalation by the anthraquinone,[57] and it permits the use of a reliable process for charge injection. Light-induced single-electron transfer to the anthraquinone group quickly generates a radical cation in the RNA/DNA hybrid duplex that is suited for migration and reaction.

(2**) A Kinetic Model for Radical Cation Migration and Reaction.** Various models have been proposed to explain long-distance electron transfer in duplex DNA.[2,6] These can be divided crudely into two classes.[5] In one class, the charge (radical cation) is delocalized through bridge orbitals formed by overlapping π-electrons of the bases. In the second class, the radical cation is localized on one base and migration occurs by thermally activated "hopping" from base-to-base.[58] Recent experimental results from ultrafast spectroscopic measurements[11] and from product analyses[9,10] require a combination of these ideas in a mechanism that we call phonon-assisted polaron-like hopping. In this mechanism, the relative rates of three generalized reactions, shown schematically in Figure 6, control the efficiency of charge transport.

The polaron is formed in response to injection of the radical cation.[9] It is a local structural distortion that relieves electron deficiency by delocalizing the radical cation over several bases. The number of bases incorporated in the polaron depends on the specific sequence. The polaron migrates by hopping, a thermally activated process, with hop lengths that also depend on the specific sequence. The rate for polaron hopping, (symbolized with the pseudo-first-order rate constant k_h) is presumed to become averaged to a nearly constant value by variation of the number of bases in the polaron and by variation of the number of bases in a hopping step. In this simplified kinetic scheme, the polaron can hop, be annihilated (k_a), or be trapped (k_t). Annihilation is a process that consumes the polaron and does not give strand cleavage; trapping is a reaction of the polaron that results in eventual (after piperidine treatment) strand cleavage. The results of the charge injection are a function of the relative magnitudes of these rate constants. This model can be used to explain our findings for the efficiency of charge transport and the reactions of radical cations in RNA/DNA duplexes.

The investigations of RNA/DNA hybrid duplex global structures in solution reveal that they are composed of an ensemble of conformers characterized as being predominantly A-form. A significant difference between A- and B-form duplexes is the stacking of the bases. Stacking affects π-electron interactions between the bases and the exposure of the bases to solvent (water). Among the significant structural differences between A- and B-form DNA is the rise per base pair, which is 2.3 and 3.4 Å, respectively, in A- and B-form. In A-form DNA the helical twist angle between successive base pairs is 32°, and in the B-form this value is increased to 36°.[59] Both of these structural differences lead to increased π-electron interaction and reduced solvent exposure for the A-form. The hybrid nucleic acid may also be bent at the A−B conformational junction.[60] The experiments reported above reveal the effect of these structural changes on the transport and reactions of base radical cations in RNA/DNA hybrid duplexes.

There are three key findings that form the basis for our analysis. First, the overall efficiency of strand cleavage in the hybrid duplexes is much lower than it is in corresponding DNA duplexes. At 20 °C there is no detectable reaction at remote GG steps in the hybrid duplexes. Charge migration is readily observed in the hybrids only when the temperature is raised to 35 °C. Second, the relative amount of strand cleavage at GG_3 in AQ-DNA(30) is approximately the same when it is hybridized either with DNA(2) or CNA(2), even though for the latter the polaron must pass through a RNA/DNA hybrid segment. Finally, the amount of strand cleavage at GG_2 (a part of the RNA/DNA region) in AQ-DNA(30)/CNA(2) is much lower than it is for GG_2 in AQ-DNA(30)/DNA(2). These results can be interpreted within the proposed kinetic model by considering the influence of structure on the relative rates of the three generalized reactions.

Trapping of the polaron at a guanine leads to strand cleavage. A major product of this reaction in duplex DNA is 7,8-dihydro-8-oxo-guanine (8-OxoG)[61] which is formed by reaction with H_2O.[62] All of the essential differences between duplex DNA and the RNA/DNA hybrids can be attributed to a reduction of the rate of this trapping reaction in the latter compared with the rates for annihilation and hopping. We associate this reduction of k_t with an additional kinetic barrier for the reaction of H_2O imposed by the more hydrophobic base stack in A-form helices. Evidence supporting this view comes from analysis of imino proton exchange rates in DNA and RNA/DNA hybrid duplexes. Exchange involves breaking the Watson−Crick hydrogen bonds and solvent penetration into the core.[63] It is slower in A-form RNA-containing duplexes than it is for B-form DNA.[64] The reduction of k_t compared with k_a, for example, accommodates the overall reduced strand cleavage efficiency in the hybrid duplexes. The temperature dependence observed in the reactions of AQ-DNA(30) can be similarly ascribed. At

(56) Breslin, D. T.; Schuster, G. B. *J. Am. Chem. Soc.* **1996**, *118*, 2311−2319.
(57) Wilson, W. D.; Ratmeyer, L.; Zhao, L.; Strekowski, L.; Boykin, D. *Biochemistry* **1993**, *32*, 4098−4104.
(58) Ly, D.; Kan, Y.; Armitage, B.; Schuster, G. B. *J. Am. Chem. Soc.* **1996**, *118*, 8747−8748.
(59) Sriram, M.; Wang, A. H.-J. In *Structure of DNA and RNA*; Hecht, S. M., Ed.; Oxford University Press: New York, 1996; pp 105−143.
(60) Selsing, E.; Wells, R. D.; Alden, C. J.; Arnott, S. *J. Biol. Chem.* **1979**, *254*, 5417−5422.
(61) Kasai, H.; Yamaizumi, Z.; Berger, M.; Cadet, J. *J. Am. Chem. Soc.* **1992**, *114*, 9692−9694.
(62) Burrows, C. J.; Muller, J. G. *Chem. Rev.* **1998**, *98*, 1109−1154.
(63) Gueron, M.; Leroy, J.-L. *Methods in Enzymol.* **1995**, *261*, 383−413.
(64) Mirau, P. A.; Kearns, D. R. *J. Mol. Biol.* **1984**, *177*, 207−227.

the lower temperature, where the CD spectrum indicates the most A-like structure, the activation barrier for reaction with H_2O is too high to overcome. At the higher temperature, where the CD spectrum reports a higher B-form content, reaction at each of the three GG steps is observed, but the efficiency is much lower in the hybrid at GG_2 where the A-form structure is centered.

The kinetic model we propose suggests that polaron-like distortions form and hop in RNA/DNA hybrid duplexes. This is reasonable since their structure is flexible, and delocalization of the radical cation will lower its energy. Although it is certain that the hopping rate constants will differ in A- and B-form structures, particularly at the A−B junction,[60] it is not primarily the magnitude of this rate that controls the reaction outcome. The results of injecting a radical cation into a RNA/DNA hybrid duplex is controlled by the relative rates of those processes that consume the polaron and result in strand cleavage.

The observed inefficient strand cleavage in the AQ-DNA/RNA hybrid duplexes has implications for understanding applications of charge transport and oxidative cleavage in RNA- and DNA-containing materials. These findings suggest that hydrophobic duplexes, or H_2O-free forms, will be superior materials for application of nucleic acids as one-dimensional conductors.[12,13] Also, comparisons of oxidative cleavage for DNA and RNA have shown that DNA is a more reactive substrate.[65−68] The 5′-GG-3′ selectivity that has been widely reported for DNA is not present in RNA. Guanine cleavage is observed selectively in only single-stranded and loop/stem junction regions of RNA, where the bases are more exposed to solvent.[69] In RNA duplexes, the nucleotide on the 3′-side of a U in a G:U wobble base pair is particularly sensitive to oxidation, with little base selectivity.[70,71] This selective cleavage has been ascribed to electron trapping at the G:U site, and is believed to be the RNA equivalent of GG cleavage in DNA. On the basis of our results, it is believed that this RNA cleavage selectivity may be due to increased H_2O accessibility at this site.

Conclusion

The primary intent of this work was to examine the influence of global structure on photoinduced radical cation transport through duplex oligonucleotides. Study of RNA/DNA hybrid duplexes permits the comparison of predominant A-form structures with B-form DNA. An electronically excited anthraquinone group, linked to the 5′-end of the DNA strand, functions as a one-electron oxidant that injects a radical cation into the duplex oligonucleotides. The transport and reactions of the radical cation were monitored as remote strand cleavage primarily at the 5′-G of GG steps after piperidine treatment. The hybrid duplexes are much less reactive than B-form DNA, but long-distance radical cation transport is observed. A kinetic model of competing reactions is proposed to accommodate the results. The reduced reactivity in the hybrid duplex is attributed to its A-like structure and explained by an increased activation barrier for reaction of H_2O with guanine radical cations.

Experimental Section

Materials and Instrumentation. Radioactive isotopes [α-^{32}P]ddATP were purchased from Amersham Bioscience. Terminal deoxynucleotidyl transferase (calf thymus) was purchased from Pharmacia Biotech and stored at −20 °C. Unmodified and 5′-end-linked anthraquinone oligonucleotides were obtained from Midland Certified Reagent Company (HPLC grade). RNA(1) and CNA(2) were purchased from Cruachem (HPLC grade). Oligonucleotide concentrations were determined by absorbance at 260 nm. UV melting and cooling curves were recorded on a Cary 1E spectrophotometer equipped with a multicell block, temperature controller, and sample transport accessory. Circular dichroism measurement was performed on a Jasco model J-720 spectropolarimeter.

Thermal Denaturation and Circular Dichroism Spectrum. Samples consisted of equimolar concentrations of DNA (RNA or CNA) oligomers (1.0−5.0 μM each) in 1 mL of 10 mM sodium phosphate buffer (pH 7.0). Thermal denaturation and circular dichroism spectra were recorded with identical samples. Thermal denaturation studies were carried out in 1 cm path length semimicro cells by monitoring sample absorbance at 260 nm. A heating/cooling rate of 0.5 °C/min was maintained. Melting temperatures were determined from the maxima of first derivative plots. Circular dichroism measurements were performed with the same samples at different temperatures (20, 30, 40, and 50 °C). Five scans were taken for each temperature.

Photocleavage Analysis. AQ-DNA oligonucleotides were radiolabeled at the 3′-end using [α-^{32}P]ddATP]and terminal deoxynucleotidyl tranferase (calf thymus). The labeling was performed by incubation of 250 pmol of AQ-DNA, 1.0 μL of [α-^{32}P]ddATP, 2.0 μL of TdT, and 2.0 μL of TdT Buffer in a total volume of 20 μL, at 37 °C for 45 min. Radiolabeled DNA was purified by 20% denaturing polyacrylamide gel. A 10 μL solution of a mixture of labeled AQ-DNA (5000 cpm) and 5 μM unlabeled AQ-DNA and DNA (RNA or CNA) in 10 mM sodium phosphate was hybridized by heating at 90 °C for 5 min, followed by slow cooling to room temperature. Samples were irradiated 1 h in 1.5 mL microcentrifuge tubes using a Rayonet photoreactor (Southern New England Ultraviolet Company) equipped with eight lamps (λ = 350 nm) at 20 or 35 °C. After irradiation, the samples were precipitated with 100 μL of cold ethanol and 0.5 μL of glycogen and dried. The products were treated with 1 M piperidine at 90 °C for 30 min, dried, and dissolved in denaturing loading buffer. The photocleavage products were separated by electrophoresis on a 20% 19:1 acrylamide:bis-acrylamide gel containing 7 M urea and detected by autoradiography.

Acknowledgment. This work was supported by grants from the National Science Foundation and the National Institute of Health, for which we are grateful.

Supporting Information Available: Autoradiogram of the gel showing the temperature dependence (PDF). This material is available free of charge via the Internet at http://pubs.acs.org.

JA9925406

(65) Kappen, L. S.; Goldberg, I. H. *Biochemistry* **1995**, *34*, 4.
(66) Lim, A. C.; Barton, J. K. *Biochemistry* **1993**, *32*, 11029−11034.
(67) Neyhart, G. A.; Cheng, C.-C.; Thorp, H. H. *J. Am. Chem. Soc.* **1995**, *117*, 1463−1471.
(68) Hecht, S. M. *Bioconjugate Chem.* **1994**, *5*, 513−526.
(69) Muller, J. G.; Rokita, S. E.; Burrows, C. J. *J. Am. Chem. Soc.* **1996**, *118*, 2320−2325.
(70) Burgstaller, P.; Hermann, T.; Huber, C.; Westhof, E.; Famulok, M. *Nucleic Acids Res.* **1997**, *25*.
(71) Burgstaller, P.; Famulok, M. *J. Am. Chem. Soc.* **1997**, *119*, 1137−1138.